Viscarello, B. R., Stein, R. L., Kusner, E. J., Holsclaw, D., & Krell, R. D. (1983) *Prep. Biochem. 13*, 57–67.
Wenzel, H. R., & Tschesche, H. (1981) *Hoppe-Seyler's Z. Physiol. Chem. 362*, 829–831.
Wright, C. S., Alden, R. A., & Kraut, J. (1972) *J. Mol. Biol. 66*, 283–289.
Zimmerman, M. A., & Ashe, B. M. (1977) *Biochim. Biophys. Acta 480*, 241–245.

Catalysis by Human Leukocyte Elastase: Proton Inventory as a Mechanistic Probe†

Ross L. Stein* and Anne M. Strimpler

Pulmonary Pharmacology Section, Department of Pharmacology, Stuart Pharmaceuticals, A Division of ICI Americas Inc., Wilmington, Delaware 19897

Hitoshi Hori and James C. Powers

School of Chemistry, Georgia Institute of Technology, Atlanta, Georgia 30332

Received July 28, 1986; Revised Manuscript Received October 24, 1986

ABSTRACT: Proton inventories (rate measurements in mixtures of H_2O and D_2O) were determined for the human leukocyte elastase catalyzed hydrolyses of thiobenzyl esters and *p*-nitroanilides of the peptides MeOSuc-Val, MeOSuc-Ala$_n$-Pro-Val (n = 0–2), and MeOSuc-Ala$_n$-Pro-Ala (n = 1 or 2). The dependencies of k_2/K_s on mole fraction of solvent deuterium for the *p*-nitroanilides are "dome-shaped" and were fit to a model that incorporates the mechanistic features of generalized solvent reorganization when substrate binds to enzyme and partial rate limitation of k_2/K_s by physical and chemical steps [Stein, R. L. (1985) *J. Am. Chem. Soc. 107*, 7768–7769]. The proton inventories for the deacylation of MeOSuc-Val-HLE and MeOSuc-Pro-Val-HLE are linear while those for the deacylation of MeOSuc-Ala-Pro-Val-HLE and MeOSuc-Ala-Ala-Pro-Val-HLE are "bowl-shaped" and could be fit to a quadratic dependence of rate on mole fraction of deuterium. These results are interpreted to suggest that the correct operation of the catalytic triad is dependent on substrate structure. Minimal substrates, which cannot interact with elastase at remote subsites, are hydrolyzed via a mechanism involving simple general-base catalysis by the active site histidine and transfer of a single proton in the rate-limiting transition state. In contrast, tri- and tetrapeptide substrates, which are able to interact at remote subsites, are hydrolyzed by a more complex mechanism of protolytic catalysis involving full functioning of the catalytic triad and transfer of two protons in the rate-limiting transition state. Finally, the proton inventories for the deacylation of MeOSuc-Ala-Pro-Ala-HLE and MeOSuc-Ala-Ala-Pro-Ala-HLE are dome-shaped and suggest that the chemical events of acyl-enzyme hydrolysis are only partially rate limiting for these reactions and that some other physical step is also partially rate limiting.

The proton inventory technique is an extension of the more routinely used solvent isotope effect; the latter is determined by measuring reaction rates in H_2O and D_2O and expressed as a ratio of rate constants, typically k_H/k_D and abbreviated here as ^Dk, while the former is determined by measuring reaction rates in mixtures of the isotopic waters and expressed graphically as the dependence of rate on the mole fraction of solvent deuterium n. The size of the solvent isotope effect and shape of the proton inventory are diagnostic of reaction mechanism [Schowen and Schowen (1982), especially pp 559–567; Venkatasubban & Schowen, 1985] and, upon detailed analysis, often lead to novel mechanistic insights (Harmony et al., 1975; Hunkapiller et al., 1976; Pollock et al., 1973; Matta & Toenjes, 1985; Stein, 1985c).

As probes of enzymic mechanisms, the solvent isotope effect and proton inventory have found their greatest use with serine hydrolases (Venkatasubban & Schowen, 1985). These enzymes catalyze the hydrolysis of amide and ester bonds via the double-displacement mechanism of Scheme I, in which E is enzyme, S is amide or ester substrate, E:S is the Michaelis complex, E-acyl is the acyl-enzyme, P_1 is the first product released (amine or alcohol), and P_2 is the second product released (carboxylic acid).

Scheme I: Acyl-Enzyme Mechanism for Reactions of Serine Hydrolases

$$E + S \underset{k_{-1}}{\overset{k_1}{\rightleftharpoons}} E{:}S \xrightarrow{k_2} E\text{-acyl} \xrightarrow{k_3} E + P_2$$
$$\downarrow P_1$$

$$k_c = k_2k_3/(k_2 + k_3) \quad (1)$$

$$K_m = K_sk_3/(k_2 + k_3) \quad (2)$$

$$K_s = (k_{-1} + k_1)/k_1 \quad (3)$$

$$k_c/K_m = k_1k_2/(k_{-1} + k_2) \quad (4)$$

† For part 6 of this series, see Stein et al. (1987). This work was supported in part by National Institutes of Health Grant HL29307.

* Address correspondence to this author at the Department of Enzymology, Merck Institute for Therapeutic Research, P.O. Box 2000, Rahway, NJ 07065.

0006-2960/87/0426-1305$01.50/0

Table I: Proton Inventories for Action of Human Leukocyte Elastase[a]

substrate	$[E]_0$ (μM)	$[S]_0$ (μM)	method[b]	mole fraction of D_2O [rate]	solvent isotope effect[c]	ΔC[d]
MeOSuc-Val-pNA	2.0	40	A	0.00 [4.34, 4.37]; 0.19 [3.87, 3.90]; 0.37 [3.55, 3.43]; 0.56 [3.43, 3.32]; 0.74 [2.76, 2.94]; 0.93 [2.348 2.31]	1.9	0
MeOSu-Pro-Val-pNA	0.28	35	A	0.00 [3.60, 3.58]; 0.19 [3.49, 3.47]; 0.37 [3.26, 3.34]; 0.56 [2.89, 2.81]; 0.74 [2.59, 2.55]; 0.93 [2.18, 2.18]	1.8	+12
MeOSuc-Ala-Pro-Val-pNA[e]	0.21	8	B	0.00 [1.141, 1.171]; 0.19 [1.073, 1.084]; 0.37 [0.983, 0.963]; 0.56 [0.850, 0.867]; 0.74 [0.716, 0.735]; 0.93 [0.600, 0.593]	2.0	+7
MeOSuc-Ala-Ala-Pro-Val-pNA[e]	0.057	2	B	0.00 [1.007, 0.992]; 0.19 [0.970, 0.984]; 0.39 [0.924, 0.945]; 0.58 [0.862, 0.880]; 0.77 [0.778, 0.768]; 0.96 [0.667, 0.680]	1.6	+21
MeOSuc-Ala-Pro-Ala-pNA[e]	0.19	77	A	0.00 [68.3, 68.6, 68.2]; 0.18 [63.5]; 0.37 [55.1]; 0.46 [53.8]; 0.74 [43.5]; 0.83 [36.9]; 0.93 [33.0, 31.5]	2.2	+12
MeOSuc-Ala-Ala-Pro-Ala-pNA[e]	0.028	42	A	0.00 [39.0, 38.7]; 0.19 [35.0, 36.8]; 0.39 [32.4, 32.8]; 0.59 [28.4, 28.0]; 0.78 [23.0, 22.7]; 0.98 [17.9, 19.1]	2.1	+15
MeOSuc-Val-SBzl	0.014	42	A	0.00 [162, 167]; 0.19 [132, 143]; 0.39 [120, 124]; 0.59 [95.6, 99.0]; 0.79 [77.2, 83.7]; 0.98 [59.1, 56.1]	2.7	0
MeOSuc-Pro-Val-SBzl	0.014	67	A	0.00 [149, 156]; 0.19 [121, 134, 110]; 0.39 [107, 105]; 0.59 [81.8, 83.7]; 0.79 [64.3, 70.6]; 0.98 [46.6, 46.4]	3.3	0
MeOSuc-Ala-Pro-Val-SBzl	0.014	70	A	0.00 [212, 204, 206]; 0.19 [167, 166, 172]; 0.39 [140, 146, 149]; 0.59 [120, 103, 110]; 0.79 [92.6, 89.2, 95.2]; 0.98 [69.2, 67.8, 68.4]	2.9	−9
MeOSuc-Ala-Ala-Pro-Val-SBzl	0.014	90	A	0.00 [203, 212, 210], 0.19 [178, 174, 176]; 0.39 [141, 139, 140]; 0.59 [124, 122, 119]; 0.79 [97.1, 95.3, 92.6]; 0.98 [78.4, 76.1, 72.5]	2.8	−8
MeOSuc-Ala-Pro-Ala-SBzl	0.007	254	A	0.00 [480, 481]; 0.19 [442, 439]; 0.39 [371, 369]; 0.59 [302, 296]; 0.79 [250, 243]; 0.98 [180, 172]	2.8	+3
MeOSuc-Ala-Ala-Pro-Ala-SBzl	0.007	276	A	0.00 [438, 447]; 0.19 [427, 419]; 0.39 [373, 383]; 0.59 [310, 305]; 0.79 [241, 255]; 0.98 [181, 192]	2.5	+13

[a] Proton inventories were conducted in 0.10 M HEPES–0.50 M NaCl, pH 7.8 and pD equivalent, at 25.0 ± 0.1 °C. [b] Method A: Initial velocity determinations; rates are expressed in units of 10^{-5} OD/s. Method B: Progress curves were recorded and fit to a first-order rate law; observed rate constants are expressed at 10^{-2} s^{-1}. [c] Error estimates for solvent isotope effects are no greater than ±0.07. [d] See eq 5. [e] Stein, 1985d.

The central feature of this mechanism is the acyl-enzyme, formed by the attack of the active site serine residue on the carbonyl carbon of the substrate. Solvent isotope effects and proton inventory experiments have been used to probe the catalytic mechanisms that stabilize the transition states for the formation and subsequent hydrolysis of this intermediate. In general, solvent isotope effects between 2 and 4 are observed for these reactions and indicate transition-state stabilization by some form of protolytic catalysis.

Proton inventories for reactions of serine proteases indicate an elaborate mechanism for this protolytic catalysis (Venkatasubban & Schowen, 1985) that is dependent on structural features of the substrate. It appears that, during the hydrolysis of specific substrates, two protons are transferred in the transition states for acylation and deacylation; during hydrolysis of nonspecific substrates, only a single proton is transferred. These results have been interpreted in the context of the "catalytic triad", an assembly of amino acid residues (Asp-102, His-57, and Ser-109; chymotrypsin numbering) shown by X-ray diffraction studies to exist at the active site of serine proteases (Blow et al., 1970; Kraut, 1977; Steitz, 1982). This interpretation claims that for specific substrates, which fulfill certain structural requirements imposed by the enzyme, the catalytic machinery of the triad is fully engaged and operates with concerted transfer of the two protons resident in the catalytic triad. For substrates that are structurally inadequate, the catalytic triad is uncoupled and operates by a simpler mechanism involving transfer of the single proton between His-57 and Ser-195. This form of catalysis resembles the general catalysis of small-molecule systems.

Solvent isotope effects and proton inventories have also been used to explore the solvent reorganization that occurs during enzymatic and nonenzymatic reactions (Matta & Andracki, 1985; Matta & Toenjes, 1985; Stein & Matta, 1985; Stein, 1985c,d) as well as the conformation changes that can occur in some enzymic reactions (Stein, 1985c; Venkatasubban & Schowen, 1985; Wang et al., 1975).

In an attempt to detect changes in mechanism that occur with systemic changes in substrate structure, we have applied these isotopic probes to the hydrolysis of a series of structurally related substrates by human leukocyte elastase (Stein et al., 1987). The results of this study indicate that rate-limiting steps and mechanisms of protolytic catalysis are strongly coupled to structural features of the substrate. A preliminary communication of a portion of this work has appeared earlier (Stein, 1985d).

Materials and Methods

HLE[1] was prepared as previously described (Stein, 1985b; Viscarello et al., 1983). Buffer salts and Me_2SO were of analytical grade from several sources. D_2O was from Sigma Chemical Co., St. Louis, MO. Substrates were available from a previous study (Stein et al., 1987). Steady-state kinetic measurements and proton inventory experiments were conducted according to established methods (Stein, 1983, 1985b; Stein et al., 1987).

Results

Proton inventories were determined for the HLE-catalyzed hydrolysis of a series of peptide *p*-nitroanilides in 0.10 M HEPES–0.50 M NaCl, pH 7.8 and pD equivalent, at 25.0 ± 0.1 °C. The data from these experiments are summarized in Table I and displayed graphically in Figure 1 for two of the substrates. Since the substrate concentration for all six *p*-nitroanilides was at least 20-fold less than their K_m values, the proton inventories are for k_c/K_m. In all cases, except MeOSuc-Val-pNA, the proton inventories have a characteristic "bowed-upward" shape. For MeOSuc-Val-pNA, the proton inventory is linear.

[1] Abbreviations: MeOSuc, methoxysuccinyl; pNA, *p*-nitroanilide; SBzl, thiobenzyl ester; HLE, human leukocyte elastase; HEPES, 4-(2-hydroxyethyl)-1-piperazineethanesulfonic acid.

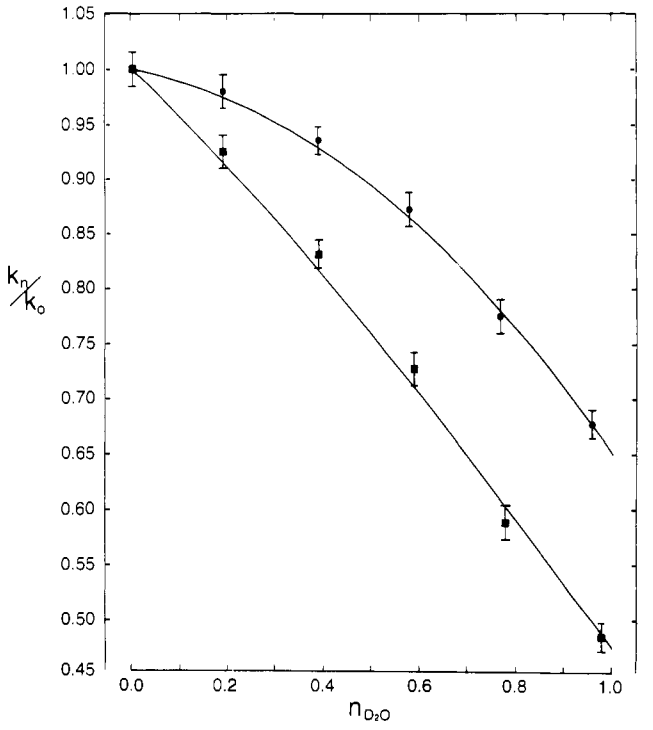

FIGURE 1: Dependence of partial solvent isotope effect on mole fraction of solvent deuterium for HLE-catalyzed hydrolysis of MeOSuc-Ala-Ala-Pro-AA-pNA (AA = Val (●) or Ala (■)). For the Val derivative, progress curves were run at $[S]_0 = 2\ \mu M$ ($0.04K_m$) and fit to a first-order rate law to obtain first-order rate constants; for the Ala derivative, initial velocities were measured at $[S]_0 = 42\ \mu M$ ($0.05K_m$). The solid line through the data for the Val substrate was drawn according to $k_n/k_0 = 1.5^n/[0.46 + 0.54/(1 - n + 0.54n)^2]$; the line through the data for the Ala substrate was drawn according to $k_n/k_0 = 1.5^n/[0.10 + 0.90/(1 - n + 0.54n)^2]$.

Also in Table I are the overall solvent isotope effects and values of ΔC (Matta & Toenjes, 1985). This latter parameter is a measure of the departure of the data from a hypothetical linear proton inventory and is calculated according to eq 5,

$$\Delta C = \frac{k_{0.5} - (k_{0.5})_{calcd}}{k_0 - k_1} \times 100 \qquad (5)$$

$$(k_{0.5})_{calcd} = k_0 - \frac{k_0 - k_1}{2}$$

where $k_{0.5}$ is the experimentally observed rate at $n = 0.5$ and $(k_{0.5})_{calcd}$ is the calculated rate at $n = 0.5$ for a linear proton inventory constructed by connecting the points in pure H_2O (k_0) and D_2O (k_1). Values of ΔC greater than 0 indicate an "upward-bowed" or dome-shaped proton inventory while negative values of ΔC indicate a "downard-bowed" or bowl-shaped proton inventory. Values of ΔC equal to 0 correspond to a linear dependence of k on n.

Proton inventories were also determined for the HLE-catalyzed hydrolyses of thiobenzyl esters that have the same acyl portions as the nitroanilides. The data for these experiments are also in Table I and are displayed in Figures 2 and 3 for MeOSuc-Ala$_x$-Pro-Val-SBzl and MeOSuc-Ala$_x$-Pro-Ala-SBzl, respectively, where x is 1 and 2. These experiments were all run at substrates concentrations much greater than K_m and thus constitute proton inventories of k_c. As indicated by their ΔC values in Table I, the proton inventories for MeOSuc-Val-SBzl and MeOSuc-Pro-Val-SBzl are linear, while those for MeOSuc-Ala$_x$-Pro-Val-SBzl (x = 1 or 2) and MeOSuc-Ala$_x$-Pro-Ala-SBzl (x = 1 or 2) are bowed downward and upward, respectively.

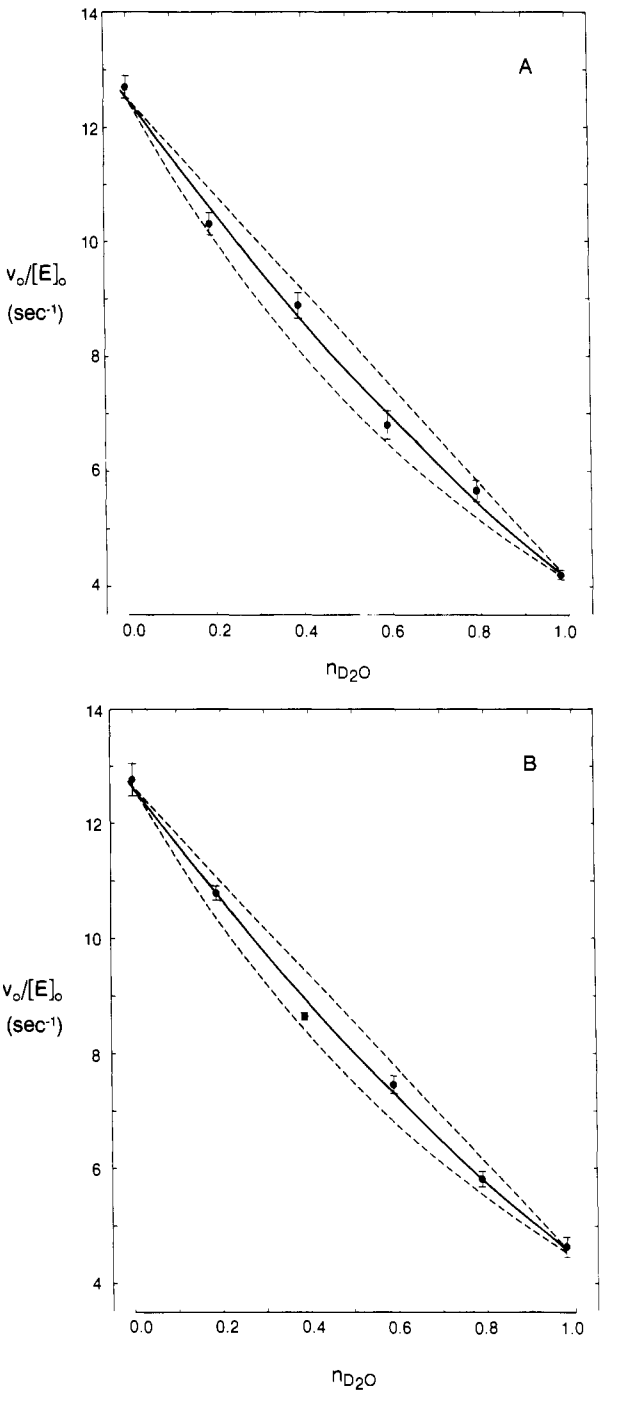

FIGURE 2: Proton inventories for HLE-catalyzed hydrolysis of MeOSuc-Ala$_x$-Pro-Val-SBzl. (A) x = 1. Initial velocities were determined at $[S]_0 = 70\ \mu M$ ($30K_m$) and divided by the $[HLE]_0$ of 14 nM. The solid line through the data was drawn according to $(v_0/[E])_n = (12.55\ s^{-1})(1 - n + 0.571n)^2$. (B) x = 2. Initial velocities were determined at $[S]_0 = 90\ \mu M$ ($40K_m$) and divided by the $[HLE]_0$ of 14 nM. The solid line through the data was drawn according to $(v_0/[E]_0)_n = (12.64\ s^{-1})(1 - n + 0.593n)^2$. For both curves, error bars are standard deviations of the mean velocity calculated from the data of Table I. The significance of the dashed lines is discussed in the text.

Steady-state kinetic parameters were determined for the HLE-catalyzed hydrolysis of MeOSuc-Ala-Pro-Ala-pNA as a function of mole fraction solvent deuterium and are summarized in Table II. Graphical presentations of the dependence of k_c, k_c/K_m, and K_m on n are shown in Figure 4. The proton inventories of k_c ($^Dk_c = 3.3 \pm 0.1$) and K_m ($^DK_m = 1.6 \pm 0.1$) are bowed downward, while that of k_c/K_m [$^D(k_c/K_m) = 2.1 \pm 0.1$] is bowed upward.

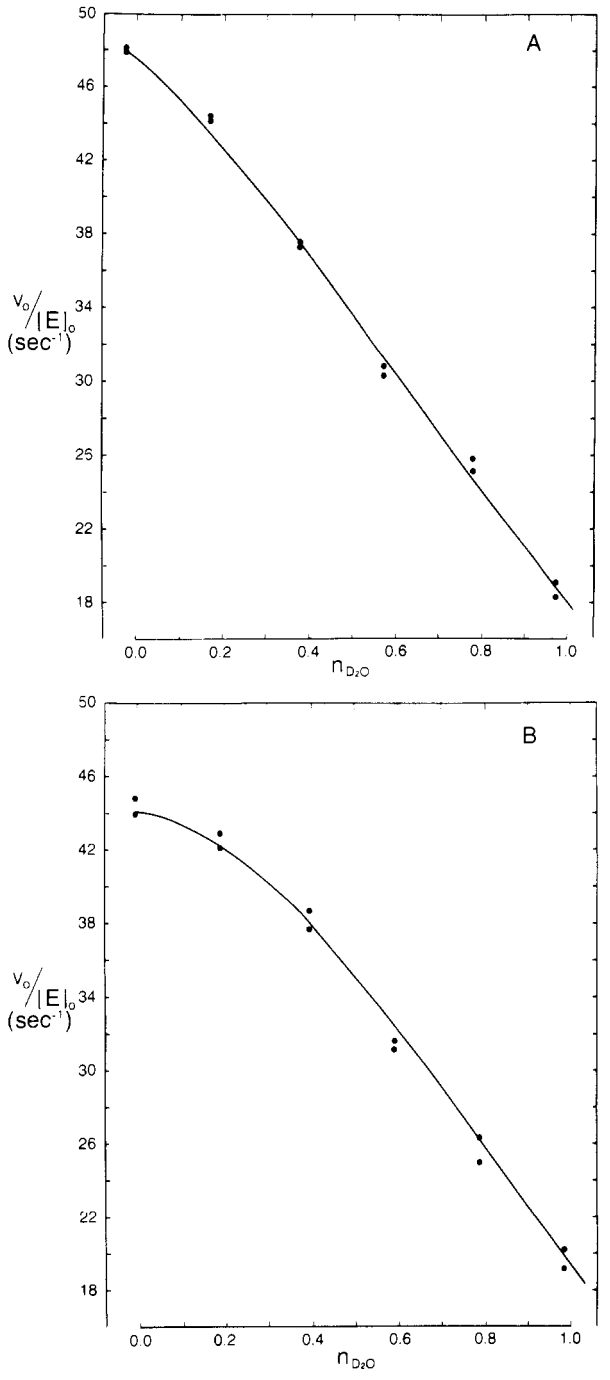

FIGURE 3: Proton inventories for HLE-catalyzed hydrolysis of MeOSuc-Ala$_x$-Pro-Ala-SBzl. (A) $x = 1$. Initial velocities were determined at $[S]_0 = 254$ μM ($20K_m$) and divided by the $[HLE]_0$ of 7 nM. The line through the data was drawn according to $(v_0/[E]_0)_n = (48\ s^{-1})/[0.25/3.7^n + 0.75/(1 - n + 0.52n)^2]$. (B) $x = 2$. Initial velocities were determined at $[S]_0 = 276$ μM ($20K_m$) and divided by the $[HLE]_0$ of 7 nM. The line through the data was drawn according to $(v_0/[E]_0)_n = (44\ s^{-1})/[0.40/4.1^n + 0.60/(1 - n + 0.52n)^2]$.

Development of Mechanistic Models for Proton Inventories of HLE

Proton inventories for reactions in which the measured rate constant reflects the free energy difference between a single reactant state and transition state can be described by the Gross–Butler equation (Venkatasubban & Schowen, 1985):

$$k_n/k_{n=0} = \frac{\prod_i^{v_T} 1 - n + n\phi_{T,i}}{\prod_j^{v_R} 1 - n + n\phi_{R,j}} \quad (6)$$

Table II: Steady-State Kinetic Parameters for Human Leukocyte Elastase Catalyzed Hydrolysis of MeOSuc-Ala-Pro-Ala-pNA Determined in Mixtures of Protium Oxide and Deuterium Oxide[a]

n_{D_2O}	k_c (s^{-1})	K_m (mM)	k_c/K_m (M^{-1} s^{-1})
0.00	7.33 ± 0.18	1.51 ± 0.07	4850 ± 140
0.24	5.52 ± 0.10	1.21 ± 0.05	4500 ± 110
0.49	4.61 ± 0.26	1.13 ± 0.06	3930 ± 80
0.74	3.11 ± 0.24	0.96 ± 0.04	3245 ± 160
0.97	2.26 ± 0.09	0.92 ± 0.05	2410 ± 120

[a] Reactions were conducted in 0.10 M HEPES–0.50 M NaCl, pH 7.75 and pD equivalent, at 25.0 ± 0.1 °C. $[HLE]_0 = 28$ nM; six substrate concentrations were used between 0.25 and 3.2 mM. Kinetic parameters and their standard deviations at each value of n_{D_2O} were determined by nonlinear least-squares fit of the initial velocity data to the Michaelis–Menten equation.

In eq 6, n is the mole fraction of solvent deuterium, v_T and v_R are the number of exchangeable protons in the transition state and reactant state, respectively, and ϕ_T and ϕ_R are the corresponding deuterium fractionation factors for the exchangeable protonic sites relative to bulk water. For serine proteases, the denominator of eq 6 is assumed to be unity (Stein, 1983; Venkatasubban & Schowen, 1985). In these situations, the entire solvent isotope effect results from fractionation of deuterium at exchangeable protonic sites of the transition state, and eq 6 is simplified to

$$k_n/k_{n=0} = \prod_i^{v_T} 1 - n + n\phi_{T,i} \quad (7)$$

Equation 7 is the starting point for our development of mechanistic models to explain the proton inventories of HLE catalysis (Stein, 1985c,d).

Proton Inventories of k_2/K_s for p-Nitroanilides. Proton inventories of k_c/K_m were bowed upward in all cases (see Figure 1 for examples) except for the hydrolysis of MeO-Suc-Val-pNA, whose proton inventory was linear. Proton inventories for HLE and related proteases having this characteristic bowed-shaped have been interpreted to reflect a mechanism in which k_c/K_m is rate-limited by more than a single transition state (Stein, 1985c,d; Stein & Matta, 1985). This mechanism is depicted in Scheme II, wherein enzyme and substrate first combine to form the Michaelis complex, E:S, which through some physical step forms yet another noncovalent complex, (E:S)′. This physical step is relatively insensitive to substrate structure and isotopic composition of the solvent (Stein, 1985b) and may represent a conformational change of E:S. Finally, the acyl-enzyme, E-acyl, is formed from (E:S)′ through a reaction step governed by k_{2b}. This scheme was first proposed as a result of pre-steady-state kinetic experiments (Stein, 1985b) and is similar to an earlier mechanism suggested by solvent isotope effect studies (Stein, 1983).

Scheme II: Acyl-Enzyme Formation for HLE

$$E + S \underset{k_{-1}}{\overset{k_1}{\rightleftharpoons}} E{:}S \underset{k_{-2a}}{\overset{k_{2a}}{\rightleftharpoons}} (E{:}S)' \xrightarrow{k_{2b}} E\text{–acyl} + P_1$$

$$k_c/K_m = k_1k_{2a}k_{2b}/[k_{-1}(k_{-2a} + k_{2b})] \quad (8)$$

When k_{-2a} and k_{2b} are similar in magnitude, k_c/K_m is not rate limited by a single transition state but rather by a "virtual" transition state (Schowen, 1978; Stein, 1981), which reflects transition-state properties of both k_{2a} and k_{2b}. An expression for the proton inventory for these reactions can be derived by starting from eq 6 and two mechanistic features of serine protease catalyzed reactions (Stein, 1985c): (i) dissociation constants of complexes formed from serine proteases and

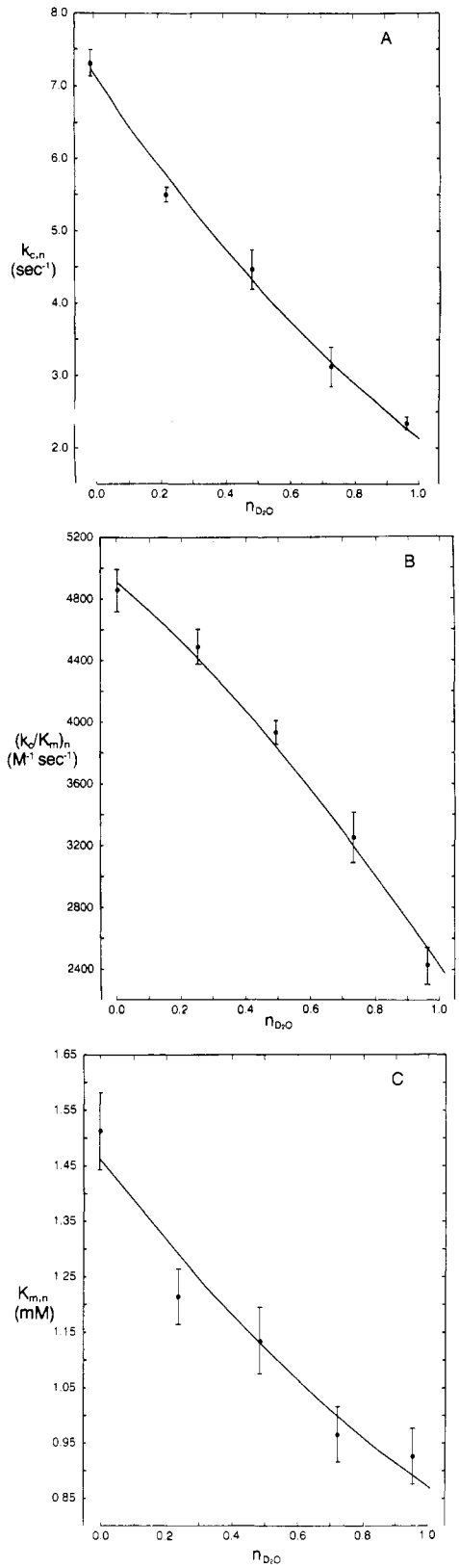

FIGURE 4: Proton inventories of steady-state kinetic parameters for HLE-catalyzed hydrolysis of MeOSuc-Ala-Pro-Ala-pNA. Initial velocities were determined at five values of n and at six concentrations of substrate between 0.25 and 3.2 mM. For each mole fraction of deuterium, the initial velocity data were fit to the Michaelis–Menten equation by nonlinear least-squares to arrive at best fit kinetic parameters for that value of n. (A) Proton inventory of k_c; line drawn according to $k_{c,n} = (7.22\ s^{-1})(1 - n + 0.54n)^2$. (B) Proton inventory of k_c/K_m; line drawn according to $(k_c/K_m)_n = (4910\ M^{-1}\ s^{-1})(1.5^n)/[0.15 + 0.85/(1 - n + 0.54n)^2]$. (C) Proton inventory of K_m; line drawn according to $K_{m,n} = (1.46\ mM)(1.5^{-n})[0.15(1 - n + 0.54n)^2 + 0.85]$.

substrates or inhibitors are frequently lower in magnitude in D_2O than in H_2O (i.e., ${}^DK_m \simeq {}^DK_i > 1$), and (ii) the transition state corresponding to k_2/K_s may be virtual. This expression was derived from eq 6 in earlier studies (Stein, 1985c,d) and is

$$\frac{(k_2/K_s)_n}{(k_2/K_s)_0} = Z_1\left[C_{2a} + \frac{C_{2b}}{(1 - n + n\phi_{T,2b})^v}\right]^{-1} \quad (9)$$

In this equation, k_2/K_s replaces k_c/K_m to emphasize the fact that the process being explored reflects both substrate binding, K_s [$=(k_2 + k_{-1})/k_1$], and acylation, k_2 [$=k_{2a}k_{2b}/(k_{-2a} + k_{2b})$]. Z_1 [Schowen and Schowen (1982), especially pp 559–567] is a composite, transition-state fractionation factor that reflects the generalized solvent reorganization that occurs during substrate binding (Kresge & Schowen, 1975). Z will be greater than 1 and similar in magnitude to dissociation constant solvent isotope effects. $\phi_{T,2b}$ is one of two transition-state fractionation factors corresponding to the two exchangeable sites of the charge-relay system. C_{2a} and C_{2b} are the transition-state contributions (Stein, 1981) made by the physical and chemical steps, respectively, to the rate determination of k_2/K_s. Finally, v is the number of protonic sites of the charge-relay system contributing to the overall isotope effect.

The two transition-state contributions, C_{2a} and C_{2b}, are expressed as

$$C_{2a} = (k_2/K_s)/k_{2a}' \quad (10)$$

$$C_{2b} = (k_2/K_s)/k_{2b}' \quad (11)$$

where $k_{2a}' = k_{2a}/K_s$, $k_{2b}' = k_{2b}/(K_sK_{2a})$, $K_s = k_{-1}/k_1$, and $K_{2a} = k_{-2a}/k_{2a}$ (Stein, 1981).

At this stage of our analysis, we would like to estimate the magnitudes of the parameters of eq 9 for the various proton inventories. As discussed previously (Stein, 1985c), however, attempts at parameter estimation for models as complex as eq 9 will invariably result in nonconvergence of the nonlinear least-squares fit. What must be done in these cases is to constrain one or more of the parameters to "realistic" values and then solve for the rest (Stein, 1985c,d). Justification of this strategy, as well as a rational procedure for assigning realistic values to constrained parameters, has been presented (Stein, 1985c).

Analyses of the proton inventories for the tri- and tetrapeptide *p*-nitroanilides of this study were reported in a preliminary paper (Stein, 1985d). Briefly, Z_1 and $\phi_{T,2b}$ were constrained to values of 1.5 and 0.54, respectively, and estimates of C_{2a} and C_{2b} were then determined by nonlinear least-squares fit of the proton inventory data to this constrained form of eq 9. The results of the fits are summarized in Table III and displayed graphically for MeOSuc-Ala-Ala-Pro-Val-pNA and MeOSuc-Ala-Ala-Pro-Ala-pNA in Figure 1. For all of these fits, v, the number of protonic sites of the charge-relay system contributing to the solvent isotope effect, was set equal to 2. Use of the squared term in eq 9 is justified by observations of proton inventories of k_2 for MeOSuc-Ala-Pro-Ala-pNA and k_3 for MeOSuc-Ala-Pro-Val-SBzl and MeOSuc-Ala-Ala-Pro-Val-SBzl, which, as will be discussed below, are "bowed downward" and are fit by the expression $k_n/k_0 = (1 - n + n\phi_T)^2$.

For the substrates MeOSuc-Val-pNA and MeOSuc-Pro-Val-pNA, v was set equal to 1. This was based on linear proton inventories of k_3 for MeOSuc-Val-SBzl and MeOSuc-Pro-Val-SBzl (see below). The proton inventory of k_2/K_s for MeOSuc-Pro-Val-pNA is bowed upward and was fit to eq 9 with the single constraint that $Z_1 = 1.5$. The linear proton

Table III: Parameter Estimates for Proton Inventories of k_2/K_s

	k_2/K_s[a]	Z_1	C_{2a}	C_{2b}	$\phi_{T,2b}$	ν
MeOSuc-Val-pNA[b]	75	1.2	0.00 ± 0.10	1.00 ± 0.10	0.42 ± 0.06	1
MeOSuc-Pro-Val-pNA[b]	575	1.5	0.00 ± 0.09	1.00 ± 0.09	0.36 ± 0.03	1
MeOSuc-Ala-Pro-Val-pNA[b]	56 000	1.5	0.14 ± 0.02	0.86 ± 0.02	0.54	2
MeOSuc-Ala-Ala-Pro-Val-pNA[b]	182 000	1.5	0.46 ± 0.01	0.54 ± 0.01	0.54	2
MeOSuc-Ala-Pro-Ala-pNA	4 500	1.5	0.05 ± 0.02	0.95 ± 0.02	0.54	2
MeOSuc-Ala-Ala-Pro-Ala-pNA	27 000	1.5	0.10 ± 0.03	0.90 ± 0.03	0.54	2

[a] Data from Stein et al. (1987) and expressed as M^{-1} s^{-1}. [b] Stein, 1985d.

Table IV: Parameter Estimates for Proton Inventories of k_3

	k_3[a]	C_{3p}	Z_{3p}	C_{3c}	$\phi_{T,3c}$	ν
MeOSuc-Val-HLE	10	0		1	0.368 ± 0.004	1
MeOSuc-Pro-Val-HLE	11	0		1	0.311 ± 0.006	1
MeOSuc-Ala-Pro-Val-HLE	13	0		1	0.57 ± 0.01	2
MeOSuc-Ala-Ala-Pro-Val-HLE	13	0		1	0.59 ± 0.01	2
MeOSuc-Ala-Pro-Ala-HLE	46	0.25 ± 0.02	3.7 ± 0.08	0.75 ± 0.02	0.52	2
MeOSuc-Ala-Ala-Pro-Ala-HLE	53	0.40 ± 0.02	4.1 ± 1.1	0.60 ± 0.02	0.52	2

[a] Data from Stein et al. (1987) and expressed in units of s^{-1}.

inventory of k_2/K_s for the hydrolysis of MeOSuc-Val-pNA was fit to eq 9 with the constraint that $Z_1 = 1.2$. Larger values of Z_1 (e.g., 1.5) resulted in estimates of C_{2a} that were negative. Parameter estimates for these experiments are in Table III.

Taken together, these results indicate that increases in substrate reactivity, as reflected in k_2/K_s, are accompanied by increases in the contribution of the physical step, k_{2a}, and decreases in the contribution of the chemical step, k_{2b}, to the rate determination of k_2/K_s. As previously suggested (Stein, 1985b,d), these changes in transition-state contributions result from stabilization of the transition state for the chemical step alone; the stability of the transition state for the physical step appears not to be sensitive to substrate structure. Finally, it is important to note that the observed trends in C_{2a} and C_{2b} are not dependent on the values to which Z_1 and $\phi_{T,2b}$ are constrained. Values of Z_1 between 1.1 and 1.7 and values of $\phi_{T,2b}$ between 0.50 and 0.60 give similar results.

Proton Inventories of k_3. Proton inventories of k_c were determined for the HLE-catalyzed hydrolysis of several thiobenzyl esters (see Table I). Since k_c is rate-limited by deacylation for these reactions (Stein et al., 1987), these proton inventories are of the deacylation rate constant, k_3. We will first consider the proton inventories for the four acyl-enzymes with Val at P_1.

For the hydrolysis of the acyl-enzymes MeOSuc-Val-HLE and MeOSuc-Pro-Val-HLE, the proton inventories are linear and consistent with deacylation mechanisms in which the observed solvent isotope effect originates entirely from deuterium fractionation at a single protonic site in the rate-limiting transition state. The data from these experiments were fit to the linear expression of eq 12. Estimates of $\phi_{T,3}$ from these

$$k_{3,n}/k_{3,0} = 1 - n + n\phi_{T,3} \qquad (12)$$

fits are given in Table IV.

In contrast to these results, the proton inventories for the hydrolyses of the acyl-enzymes MeOSuc-Ala-Pro-Val-HLE and MeOSuc-Ala-Ala-Pro-Val-HLE are both bowed downward. These curves were fit to the quadratic expression of eq 13. The results of these fits are summarized in Table IV and

$$k_{3,n}/k_{3,0} = (1 - n + n\phi_{T,3})^2 \qquad (13)$$

displayed graphically in Figure 2. The straight dashed lines connect the data points in pure light and heavy water and represent the proton inventory that would have been obtained if transfer of a single proton generated the isotope effects. The curved dashed lines were generated from a model in which transfer of four protons generated the isotope effect. Thus, for the hydrolyses of these two acyl-enzymes, the solvent isotope effects appear to involve deuterium fractionation at two (or possibly three) protonic sites in the rate-limiting transition state.

The interpretation just presented for these four proton inventories is consistent with a large and growing body of literature (Elrod et al., 1980; Hunkapiller et al., 1976; Quinn et al., 1980; Pollock et al., 1973; Stein et al., 1983; Stein, 1983; Venkatasubban & Schowen, 1985) that documents that linear proton inventories of k_c, which suggest one-proton catalysis, will be observed for serine protease catalyzed hydrolyses of nonspecific substrates, while bowed-downward curves that fit a quadratic model and suggest two-proton catalysis will be seen for specific substrates.

The proton inventories for the hydrolyses of MeOSuc-Ala-Pro-Ala-HLE and MeOSuc-Ala-Ala-Pro-Ala-HLE present a more complex situation. Both proton inventories are curved upward (Figure 3), dramatically so for the tetrapeptide, and thus suggest rate limitation of deacylation by a virtual transition state and the mechanism of Scheme III. In this scheme, P_2 is the peptide product and (E*acyl) is either a noncovalent, binary complex of enzyme and peptide or a conformer of the acyl-enzyme. If (E*acyl) is a complex of enzyme and product, then k_{3a} and k_{3b} are the first-order rate constants for deacylation and enzyme–product dissociation, respectively. However, if (E*acyl) is a conformer of the acyl-enzyme, then k_{3a} and k_{3b} correspond to a conformation change of the acyl-enzyme and deacylation, respectively.

Scheme III: Hydrolysis of Acyl-Enzymes of HLE

$$\text{E–acyl} \underset{k_{-3a}}{\overset{k_{3a}}{\rightleftharpoons}} \text{(E*acyl)} \xrightarrow{k_{3b}} \text{E} + \text{P}_2$$

Since at this time we do not know the identity of (E*acyl), the general model of eq 14, which is analogous to eq 9, was derived to account for these proton inventories:

$$\frac{k_{3,n}}{k_{3,0}} = \left[\frac{C_{3p}}{Z_{3p}} + \frac{C_{3c}}{(1 - n + n\phi_{T,3c})^2} \right]^{-1} \qquad (14)$$

In this equation, C_{3p} and C_{3c} are the transition-state contributions made by physical and chemical steps to the rate limitation of k_3. For both models the chemical step corresponds to deacylation, while the physical step varies with the identity of (E*acyl). If this species is a binary complex of enzyme and

product, the physical step corresponds to dissociation of an enzyme–product complex, while if (E*acyl) is a conformer of E-acyl, then the physical step corresponds to a conformational change. Z_{3p} is analogous to Z_1 and reflects generalized solvent reorganization as well as any other isotopic fraction caused by the physical step (stein, 1985c). $\phi_{T,3c}$ reflects deuterium fractionation by the charge-relay system in the transition state for deacylation, and v is the number of active protons. Note that this model can also account for the proton inventories of k_3 for the substrates with Val at P_1 if C_{3p} is set equal to 0 (see Table IV).

The data for the proton inventories for the hydrolyses of MeOSuc-Ala-Pro-Ala-HLE and MeOSuc-Ala-Ala-Pro-Ala-HLE were fit to eq 14 with $\phi_{T,3c}$ constrained to 0.52. Parameter estimates are summarized in Table IV and indicate that the physical step makes a larger contribution to the rate determination of k_3 for the tetrapeptide than for the tripeptide. The significance of this result, as well as the large value of Z that accompanies the physical step, will be discussed later.

Proton Inventories for Hydrolysis of MeOSuc-Ala-Pro-Ala-pNA. The proton inventory of k_c for the HLE-catalyzed hydrolysis of MeOSuc-Ala-Pro-Ala-pNA is bowed downward (Figure 4A) and thus suggests two-proton catalysis in the rate-limiting transition step for this reaction. Results from previous studies indicate that for the hydrolysis of this substrate $k_2 \ll k_3$, and thus k_2 rate limits k_c (Stein et al., 1987). Furthermore, in this study we have demonstrated that k_2 is rate-limited by the chemical steps of acylation, k_{2b}, to the extent of about 95% (Table III). These factors justified fitting the data of this proton inventory to the simple expression of eq 15. A value of $\phi_{T,c} = 0.54 \pm 0.02$ was determined and

$$k_{c,n}/k_{c,0} = (1 - n + n\phi_{T,2b})^2 \quad (15)$$

was used, along with eq 15, to draw the solid line in Figure 4A.

The proton inventory of k_c/K_m for the HLE-catalyzed hydrolysis of this substrate is bowed upward (Figure 4B) and was fit to eq 9 with Z_1 and $\phi_{T,2b}$ constrained to 1.5 and 0.54, respectively. Estimates of C_{2a} and C_{2b} determined from this fit are 0.15 ± 0.07 and 0.85 ± 0.07, respectively, in fair agreement with previously determined estimates of these parameters (Table II). The solid line of Figure 4B was according to eq 9 and these parameters.

The proton inventory of K_m for the reaction of HLE and MeOSuc-Ala-Pro-Ala-pNA was also determined and found to be bowed downward (Figure 4C). Division of eq 15 by eq 9 yields an expression for the proton inventory of K_m:

$$K_{m,n}/K_{m,0} = Z^{-n}[C_{2a}(1 - n + n\phi_{T,2b})^2 + C_{2b}] \quad (16)$$

Figure 4C contains the data for this proton inventory and the line drawn according to eq 16 and the parameter estimates given above.

Discussion

The proton inventories of this study were conducted to explore the sensitivity of various mechanistic features of HLE to systematic changes in substrate structure. We find that two features of HLE's mechanism are sensitive to substrate structural variation: charge-relay catalysis and structural features of virtual transition states.

Charge-Relay Catalysis. Proton inventories of k_2 and k_3 for a number of serine protease catalyzed reactions have been interpreted in the context of charge-relay catalysis (Elrod et al., 1980; Hunkapiller et al., 1976; Quinn et al., 1980; Pollock et al., 1973; Stein et al., 1983; Stein, 1983; Venkatasubban & Schowen, 1985). Linear proton inventories have been found for minimal, nonspecific substrates that lack critical structural features for effective transition-state interactions with the protease and have been said to signal a malfunctioning of the catalytic triad. During hydrolysis of these substrates, only one-proton catalysis, mediated by the active site His, is observed. In contrast, bowed-downward proton inventories have been found for the hydrolysis of specific substrates that more completely satisfy structural requirements imposed by the protease. The interpretation here is that these substrates establish intimate interactions with the enzyme in catalytic transition states and, in so doing, cause the charge-relay system to operate with the coupled transfer of two protons.

The mechanistic picture outlined above raises a number of important questions concerning the proton inventory technique and the charge-relay system, in general, and leukocyte elastase, in particular. The questions we will address are as follows: (1) Are there other relevant interpretations of proton inventory data? (2) Is there a structural basis for communication between remote subsites and the catalytic triad? (3) What mechanism of proton transfer can account for the solvent isotope effects observed during serine protease catalysis? (4) Do stable-state probes and transition-state probes of serine proteases support a common mechanism of catalysis? (5) What are HLE's substrate structural requirements for operation of its charge-relay system? (6) What contribution to HLE's overall catalytic efficiency is made by the charge-relay system?

(1) The first question concerns the possibility of interpretations of proton inventory data other than those just provided. In the context of this discussion of charge-relay catalysis, we are specifically asked to identify mechanisms that give rise to bowed-downward proton inventories. It is important to consider this question since it is a well-known shortcoming of proton inventories that they are usually consistent with several mechanistic models (Venkatasubban & Schowen, 1985). However, in cases of bowed-downward proton inventories, the mechanistic possibilities we need to consider are limited, since these curves can *only* be explained by mechanisms that involve the transfer of two or more protons in a single rate-limiting transition state. Reactions having virtual transition states, composed of transition states from several partially rate limiting steps, cannot generate bowed-downward proton inventories if each contributing transition state involves transfer of no more than one proton. Rather, these reactions will generate bowed-upward, or dome-shaped, proton inventories for mechanisms involving serial reaction steps or linear proton inventories for mechanisms involving parallel reactions steps. We see then that, for a reaction that generates a bowed-downward proton inventory, we know with certainty that the mechanism for this reaction involves transfer of multiple protons in the rate-limiting transition state.

Another point of interpretation we need to consider is the assignment of the physical site of proton fractionation. Like all kinetic techniques, the proton inventory is handicapped in that it can provide no structural information: although we may be able to determine the number of active protons, we cannot determine the site of their transfer. For serine proteases, however, we are fortunate in that X-ray crystallographic studies have revealed three areas on the enzyme surface where the transfer of a small number of protons in catalytic transition states could occur: (i) remote subsites, (ii) the "oxyanion hole" (Kraut, 1977), and (iii) the catalytic triad.

The first alternative predicts that as substrates are elaborated to interact at remote subsites, bowed-downward proton inventories will be observed due to the multiple hydrogen bonds that are formed in the catalytic transition states for these

reactions. Substrates that cannot bind at remote subsites will obviously not participate in these hydrogen bonds and will therefore be observed to have linear proton inventories, presumably due to general catalysis by the active site His. This hypothesis can be rejected on the basis of two considerations. First, we observe a linear proton inventory of k_2 for Suc-Ala-Ala-Ala-pNA (Stein, 1983) but a bowed-downward proton inventory of k_2 for MeOSuc-Ala-Pro-Ala-pNA. Both substrates occupy subsites S_4 through S_1' and should form a similar number of hydrogen bonds in their transition states for acylation. The proton inventories for both reactions should be bowed downward if hydrogen bonds at remote subsites generate isotope effects.

The second consideration is that the proton inventory for the hydrolysis of neither MeOSuc-Ala-Pro-Val-HLE nor MeOSuc-Ala-Ala-Pro-Val-HLE can be accurately described by models having more than two or three transition-state proton bridges. This is illustrated by bowed-downward dashed lines of panels A and B of Figure 2, which represent models in which a very large number of proton bridges (i.e., four or more) generate the observed isotope effects. Clearly, the experimental data cannot be described by this model. Furthermore, the data were fit by a polynomial regression method to determine the statistical significance, by an F test, of each additional polynomial term, or proton bridge [Schowen and Schowen (1982), especially pp 559–567; Venkatasubban & Schowen, 1985]. For the proton inventory of MeOSuc-Ala-Ala-Pro-Val-HLE deacylation, the linear and quadratic terms are significant at the 99.9% confidence level, while cubic and higher terms are significant at less than an 80% confidence level. Similarly, for MeOSuc-Ala-Pro-Val-HLE the linear and quadratic terms are significant at the 99.9% confidence level, the cubic term is significant at the 90% confidence level, and quartic and higher terms are significant at less than an 80% confidence level. These results are consistent with at least two but no more than three proton bridges in the rate-limiting transition states for hydrolysis of tri- and tetrapeptide acyl-enzymes of HLE. Combined with the previous consideration, these results strongly suggest that the establishment of hydrogen bonds at remote subsites does not generate the isotope effects that cause the downward curvature observed in deacylation proton inventories.

Another potential site for the multiple proton transfer seen with specific substrates is the oxyanion hole. The oxyanion hole is a structural unit at the active site of serine proteases that is thought to participate in stabilizing acyl-transfer transition states via hydrogen bonds from two protein backbone amide groups to the oxyanion that exists during the formation and collapse of tetrahedral intermediates. In transition states for specific substrates, the hydrogen bonds of the oxyanion hole would couple with the single proton transfer at the active site histidine to generate bowed-downward proton inventories. Although we cannot exclude this possibility at this time, it is not clear that the hydrogen bonds at work in the oxyanion hole would constitute sites of proton fractionation and generate isotope effects.

The site of proton fractionation we favor is the catalytic triad. Its mode of operation and dependence on substrate structure are presented below.

(2) We next address the second question asked in the introduction to this section and consider how remote subsites could communicate with catalytic residues. Extended peptide substrates have been shown to bind to serine proteases by forming an antiparallel β-sheet hydrogen-bonding system between the peptide backbone of residues 214, 215, and 216 and the P_1–P_3 residues of the substrate (Kraut, 1977). Since one face of the S_1 pocket is composed of the peptide backbone of residues 214, 215, and 216 and some of the side chains of these residues, it is not unreasonable to conclude that binding of amino acid residues at remote subsites could subtly affect interactions at S_1 and vice versa. It is also significant that the side chain of Ser-214 is hydrogen-bonded to Asp-102 of the catalytic triad. Thus, it is clear that there are direct structural linkages between the catalytic triad, the S_1 pocket, and the peptide backbone, which is a portion of several remote subsites. The binding of the peptide aldehydes chymostatin and Ac-Pro-Ala-Pro-Phe-H to *Steptomyces griseus* protease A is one clear-cut example where the geomtry of the catalytic residues is affected by residues other than P_1 (James et al., 1980; Delbaere & Brayer, 1985). Both aldehydes have a P_1 phenylalaninal residue and bind to this serine protease by forming a tetrahedral hemiacetal adduct with the catalytic serine. In the case of chymostatin, which has a P_2 leucine, the catalytic histidine is unchanged from the position found in the native enzyme. However, in the case of the Ac-Pro-Ala-Pro-Phe-H complex, the catalytic histidine is ejected into the surrounding solvent as a consequence of prohibitively close contacts between the tetrahedral hemiacetal and the imidazole ring of His-57. These close contacts do not occur in the chymostatin complex since the aldehyde peptide chain is shifted away from His-57 due to a favorable interaction of the P_2 leucine with the S_2 subsite of the enzyme. Since these hemiacetal aldehyde adducts are similar to the tetrahedral intermediate formed during substrate hydrolysis, the results clearly point out the importance of binding effects remote from the catalytic site on events that occur during enzymatic catalysis.

(3) The third question that we consider asks: What mechanism of proton transfer can account for the solvent isotope effects and proton inventories observed for serine proteases? The original mechanism proposed by Blow, Birktoft, and Hartley in 1970 involved a preequilibrium transfer of the two protons that reside in the charge-relay system and generation of a serine alkoxide anion. This mechanism has been questioned due to the thermodynamic problem of generating an alkoxide anion at physiologic pH (Kraut, 1977). In addition, solvent isotope effects for serine protease catalysis, which are typically between 2 and 4, are also at odds with such a preequilibrium process, which would generate an isotope effect near 1.

More realistic proposals for the operation of the catalytic triad must involve some form of protolytic catalysis in which transition-state proton bridges are formed that are capable of generating isotope effects between 2 and 4. The small magnitudes of these isotope effects suggest that the proton rearrangement in these reactions is probably not part of the reaction coordinate but rather that the mechanism involves "solvation catalysis" (Kershner & Schowen, 1971, 1972; Swain et al., 1965). For reactions that involve solvation catalysis, transition states are stabilized by stronger than normal hydrogen bonds between the reactant, which is undergoing heavy atom rearrangement, and the catalyst. The protons of these hydrogen bonds lack reaction coordinate motion; that is, they are not "in flight" and are therefore predicted to generate small isotope effects.

(4) The fourth question asks if stable-state probes, such as NMR and X-ray diffraction, and transition-state probes, such as the proton inventory, support the same mechanism for serine protease catalysis. X-ray and neutron diffraction and NMR studies of serine proteases, either uncomplexed or bound to substrates or inhibitors, indicate that catalytic amino acid residues behave independently of each other and possess no unusual chemical properties (Kraut, 1977; Kossiakoff &

Spencer, 1981; Steitz, 1982). Frequently, these results have been erroneously interpreted to indicate that coupled proton transfer within the catalytic triad cannot occur during catalysis. As has been pointed out previously (Stein, 1983; Stein et al., 1983), the error of this argument is to draw conclusions about catalysis and mechanisms of transition-state stabilization from stable-state probes. It is impossible for probes of enzymic stable states to report structure features of transition states.

The fact of the matter is that NMR and diffraction studies, together with proton inventory studies, provide a single mechanistic picture for serine protease catalysis. The stable-state probes tell us that, in protease reaction ground states, the catalytic triad is uncoupled and inoperative, while the transition-state probes report coupled proton transfer and full functioning of the triad. This is, of course, the expected result: enzymic catalytic machinery has evolved for transition-state stabilization alone (Fersht, 1974; Schowen, 1978).

(5) The fifth question asked concerns HLE's substrate structural requirements for effective operation of its catalytic triad. A previous study from this laboratory (Stein, 1983) explored this aspect of HLE's mechanism by determining proton inventories for reactions of three peptide *p*-nitroanilides and found linear proton inventories for Suc-Ala-Ala-Ala-pNA and Suc-Ala-Ala-Val-pNA and a bowed-downward, quadratic proton inventory for MeOSuc-Ala-Ala-Pro-Val-pNA. These results were interpreted to suggest that only the more specific and reactive tetrapeptide substrate possesses the structural determinants necessary for functioning of the charge-relay system. We chose herein to further explore HLE's substrate requirements with a more systematically varied series of substrates.

For the hydrolysis of the series of acyl-enzymes MeOSuc-Val-HLE, MeOSuc-Pro-Val-HLE, MeOSuc-Ala-Pro-Val-HLE, and MeOSuc-Ala-Ala-Pro-Val-HLE, our results indicate that only the acyl-enzymes of the tri- and tetrapeptides are hydrolyzed with two-proton catalysis and suggest that enzyme subsites at and beyond S_3 need to be occupied to engage the catalytic triad. The monomeric and dipeptide substrates are unable to interact with HLE at these subsites and are hydrolyzed by a mechanism involving one-proton catalysis and the catalytic involvement of only the active site histidine.

Our results further suggest that the amino acid residue that occupies subsite S_1, the "specificity pocket", may not be of critical importance since both MeOSuc-Ala-Pro-Ala-HLE and MeOSuc-Ala-Ala-Pro-Ala-HLE, as well as the analogous acyl-enzymes with Val at P_1, are all hydrolyzed with two-proton catalysis. Finally, a Pro at position P_2 of the substrate may also be important for functioning of the charge-relay system. This is suggested from the proton inventories of k_2 for the hydrolyses of Suc-Ala-Ala-Ala-pNA (Stein, 1983) and MeOSuc-Ala-Pro-Ala-pNA; the former proton inventory is linear while the latter is bowed downward and quadratic. This is, of course, not a firm comparison, since the substrates do not have the same *N*-acyl groups.

(6) The final question that was posed in the introduction to this section asks if the charge-relay system is a factor in determining overall catalytic efficiency. As noted above, the acyl-enzymes MeOSuc-Val-HLE and MeOSuc-Pro-Val-HLE hydrolyze with one-proton catalysis and uncoupled function of the catalytic triad, while MeOSuc-Ala-Pro-Val-HLE and MeOSuc-Ala-Ala-Pro-Val-HLE hydrolyze with two-proton catalysis and coupled function of the catalytic triad. Despite this difference in catalytic mechanism, there is essentially no difference in deacylation hydrolytic rate constants. On the other hand, during acylation, Suc-Ala-Ala-Ala-pNA reacts with HLE with a value of k_2 of 0.6 s^{-1} and one-proton catalysis (Stein, 1983), while MeOSuc-Ala-Pro-Ala-pNA acylates HLE with k_2 equal to 7 s^{-1} (Stein et al., 1987) and two-proton catalysis. This change in acylation rate constant corresponds to a transition-state stabilization energy of about 1.5 kcal/mol. It is tempting to attribute this additional increment of stabilization energy to charge-relay catalysis. However, in light of the deacylation data, it still "remains to be established whether coupling of the charge-relay system gives rise to any substantial acceleration or if perhaps it is a mere structural and dynamic coincidence that it is coupled with physiological substrates but not with small substrates" (Maggiora & Schowen, 1977).

Structural Features of Virtual Transition States. We have previously presented results that support the existence of a virtual transition state during the acylation of HLE (Stein, 1983, 1985b–d; Stein & Matta, 1985). The mechanism consistent with these results is shown in Scheme II. An important feature of this mechanism is the involvement of a reversible step whose rate constants, k_{2a} and k_{-2a}, are independent of substrate structural features and isotopic composition of the solvent. Although we do not know the process this step represents, we believe it may be a conformational change of the Michaelis complex that aligns the substrate and the catalytic groups of the active site for effective interaction in the transition state for acylation. This hypothesis is consistent with the observation that HLE manifests specificity kinetically in acylation and not in substrate binding (Stein et al., 1987) and has been proposed previously to explain similar substrate specificity observed for the acid protease pepsin (Fruton, 1976).

There is considerable structural information for other serine proteases that indicates that subtle conformational changes occur between the Michaelis complex and the acyl-enzyme (Kraut, 1977). In the case of chymotrypsin, the indolyl ring of the acyl-enzyme (indolylacryloyl)chymotrypsin lies 0.5–1.0 Å deeper into the S_1 pocket than does the corresponding indoyl ring in the simple Michaelis complex with *N*-formyl-Trp. With subtilisin, peptides such as Z-Gly-Gly-Tyr, which correspond to the acylating portion of good substrates, bind 1 Å further out toward the enzyme surface than covalent peptide inhibitors, even though both form an antiparallel β-sheet structure with the peptide backbone of residues 214–216. In particular, the S_1–P_1 hydrogen-bond distance is too long to make a normal interaction, and the P_1 tyrosine does not fit all the way into the S_1 specificity crevice. Thus, it is possible that the physical step contributing to the virtual transition state observed during HLE acylation corresponds to a "tightening" of the Michaelis complex, resulting in a better S_1–P_1 hydrogen bond and a deeper fit of the P_1 side chain into the S_1 pocket.

Quite unexpectedly, our results also point to a virtual transition state for deacylation. The involvement of a virtual transition state during deacylation is based on dome-shaped proton inventories for the hydrolyses of MeOSuc-Ala-Pro-Ala-HLE and MeOSuc-Ala-Ala-Pro-Ala-HLE. In the absence of reactant-state fractionation factors, dome-shaped proton inventories signal mechanisms that involve partially rate limiting serial reaction steps and a virtual transition state. We propose that, for the substrates with Ala at P_1, the chemical steps of acyl-enzyme hydrolysis are sufficiently rapid to expose a physical step, while for substrates with Val at P_1 deacylation chemistry is slow relative to this physical step and entirely rate limits the process governed by k_3. We believe that this physical process corresponds to either a conformational change or the release of the peptide acid product.

Another interesting mechanistic feature that emerges from

analysis of the proton inventories for the hydrolysis of MeO-Suc-Ala-Pro-Ala-HLE and MeOSuc-Ala-Ala-Pro-Ala-HLE is the very large Z term that is associated with the partially rate limiting physical step. A Z term of similar magnitude was observed during the association of α_1-protease inhibitor with porcine pancreatic elastase (Stein, 1985c) and was interpreted as originating from general solvent reorganization that occurs as the transition state for a partially rate limiting conformational change is reached. A similar interpretation can be put forward here. Thus, the physical step we observe during the deacylation of P_1 Ala substrates would be a protein conformational change that either (i) precedes the chemical events of deacylation, (ii) precedes and facilitates release of second product, or (iii) accompanies the release of the second product. Like the association of α_1-protease inhibitor with procine elastase, this conformational change would be accompanied by general solvent reorganization that gives rise to a Z term of significant magnitude. Note that Z terms of the appropriate magnitude can be produced if as few as 20 water–protein or protein–protein hydrogen bonds tighten in the transition state for the conformational change, with each generating an inverse isotope effect of only 0.94.

Registry No. HLE, 9004-06-2; MeOSuc-Val-pNA, 106436-09-3; MeOSuc-Pro-Val-pNA, 106436-07-1; MeOSuc-Val-SBzl, 106436-10-6; MeOSuc-Pro-Val-SBzl, 106436-08-2; MeOSuc-Ala-Pro-Val-SBzl, 106436-06-0; MeOSuc-Ala-Ala-Pro-Val-SBzl, 72252-92-7; MeOSuc-Ala-Pro-Ala-SBzl, 106436-05-9; MeOSuc-Ala-Ala-Pro-Ala-SBzl, 106436-04-8; MeOSuc-Ala-Pro-Ala-pNA, 99267-44-4; MeOSuc-Ala-Ala-Pro-Ala-pNA, 99232-64-1.

References

Blow, D. M., Birktoft, J. J., & Hartley, B. S. (1970) *Nature (London) 221*, 337–339.

Delbaere, L. T. J., & Brayer, G. D. (1985) *J. Mol. Biol. 183*, 89–103.

Elrod, J. P., Hogg, J. L., Quinn, D. M., Venkatasubban, K. S., & Schowen, R. L. (1980) *J. Am. Chem. Soc. 102*, 3917–3922.

Fersht, A. R. (1974) *Proc. R. Soc. London, B 187*, 397–407.

Fruton, J. S. (1976) *Adv. Enzymol. Relat. Areas Mol. Biol. 44*, 1–36.

Harmony, J. A. K., Himes, R. H., & Schowen, R. L. (1975) *Biochemistry 14*, 5379–5386.

Hunkapiller, M. W., Forgac, M. D., & Richards, J. H. (1976) *Biochemistry 15*, 5581–5588.

James, M. N. G., Sielecki, A. R., Brayer, G. D., Delbaere, L. T. J., & Bauer, C. A. (1980) *J. Mol. Biol. 144*, 43–88.

Kershner, L. D., & Schowen, R. L. (1971) *J. Am. Chem. Soc. 93*, 2014–2024.

Kossiakoff, A. A., & Spencer, S. A. (1981) *Biochemistry 20*, 6462–6474.

Kraut, J. (1977) *Annu. Rev. Biochem. 46*, 331–358.

Kresge, A. J., & Schowen, R. L. (1975) *Faraday Symp. Chem. Soc. 10*, 166.

Maggiora, G. M., & Schowen, R. L. (1977) in *Bioorganic Chemistry* (van Tamelen, E. E., Ed.) Vol. 1, Academic, New York.

Matta, M. S., & Andracki, M. E. (1985) *J. Am. Chem. Soc. 107*, 6036–6039.

Matta, M. S., & Toenjes, A. A. (1985) *J. Am. Chem. Soc. 107*, 7591–7596.

Pollock, E., Hogg, J. L., & Schowen, R. L. (1973) *J. Am. Chem. Soc. 95*, 968.

Quinn, D. M., Elrod, J. P., Ardis, R., Friesen, P., & Schowen, R. L. (1980) *J. Am. Chem. Soc. 102*, 5358–5365.

Schowen, K. B., & Schowen, R. L. (1982) *Methods Enzymol. 87*, 551–606.

Schowen, R. L. (1972) *Prog. Phys. Org. Chem. 9*, 275–332.

Schowen, R. L. (1978) in *Transition States of Biochemical Processes* (Gandour, R. D., & Schowen, R. L., Eds.) pp 77–114, Plenum, New York.

Stein, R. L. (1981) *J. Org. Chem. 46*, 3328–3330.

Stein, R. L. (1983) *J. Am. Chem. Soc. 105*, 5111–5116.

Stein, R. L. (1985a) *Arch. Biochem. Biophys. 236*, 677–680.

Stein, R. L. (1985b) *J. Am. Chem. Soc. 107*, 5767–5775.

Stein, R. L. (1985c) *J. Am. Chem. Soc. 107*, 6039–6042.

Stein, R. L. (1985d) *J. Am. Chem. Soc. 108*, 7768–7769.

Stein, R. L., & Matta, M. S. (1985) *Fed. Proc., Fed. Am. Soc. Exp. Biol. 44*, 1055.

Stein, R. L., & Trainor, D. A. (1986) *Biochemistry 25*, 5414–5419.

Stein, R. L., Elrod, J. P., & Schowen, R. L. (1983) *J. Am. Chem. Soc. 105*, 2446–2452.

Stein, R. L., Viscarello, B. R., & Wildonger, R. A. (1984) *J. Am. Chem. Soc. 106*, 796–798.

Stein, R. L., Strimpler, A. M., Hori, H., & Powers, J. C. (1987) *Biochemistry* (preceding paper in this issue).

Steitz, T. A., & Shulman, R. G. (1982) *Annu. Rev. Biophys. Bioeng. 11*, 419–444.

Swain, C. G., Kuhn, D. A., & Schowen, R. L. (1965) *J. Am. Chem. Soc. 87*, 1553–1561.

Venkatasubban, K. S., & Schowen, R. L. (1985) *CRC Crit. Rev. Biochem. 17*, 1–44.

Viscarello, B. R., Stein, R. L., Kusner, E. J., Holsclaw, D., & Krell, R. D. (1983) *Prep. Biochem. 13*, 57–67.

Wang, M. S., Gandour, R. D., Rodgers, J., Haslam, J. L., & Schowen, R. L. (1975) *Bioorg. Chem. 4*, 392–406.